Indian Journal of Pure & Applied Physics
Vol. 62, February 2024, pp. 155-163
DOI: 10.56042/ijpap.v62i2.7956

Design and Simulation of Nanorod-Based SAW Gas Sensor to detect Hazardous Gases

Basudeba Behera* & Srushti Bhatkar

Department of Electronics and Communication Engineering, National Institute of Technology Jamshedpur, Jharkhand 831 014, India

Received 10 January 2024; accepted 22 January 2024

The work presents the design, a 2D and 3D finite element method (FEM) simulation, analysis, and optimization of a surface acoustic wave (SAW) based gas sensor. The simulation of SAW gas sensors with and without the presence of nanorods is performed. Gas adsorption on a surface causes a change in the mass, modulus, and conductivity of the sensing layer, which can be accurately, detected using SAW-based gas sensors. The device is constructed using a YZ-cut lithium niobate as a substrate, which is covered by a 0.2 μm thick intermediate layer upon which ZnO nanorods are present operating at 4 μm wavelength. Simulations in COMSOL Multiphysics are performed using eigen frequency, time-dependent, and frequency domain analysis. The materials of the intermediate layer as well as interdigitated transducers (IDTs) and the height of the nanorods are varied for the optimization of the device. The frequency shift and total displacement were seen to be significantly improved for the nanorod-based SAW gas sensor device.

Keywords: FEM; Lithium niobate; Nanorods; SAW; Gas sensor

1 Introduction

A surface acoustic wave (SAW) travels along just the surface of materials while along the depth of the device or material, the amplitude of this SAW wave decays exponentially[1]. A SAW device is generally made up of a piezoelectric substrate upon which Interdigitated Transducers (IDTs) are present. The principle on which SAW devices are based can be either a delay line model, single port resonator, or two port resonator model[2]. As can be seen in Fig. 1 (a) a SAW delay line device consists of a piezoelectric substrate, IDTs, and absorber[3]. Generally, the piezoelectric substrate maybe Lithium Niobate ($LiNbO_3$), Lithium Tantalate, or quartz. There are a pair of IDTs *i.e.*, input and output IDTs which are parted by a distance and consist of absorbers at the ends of the device. These IDTs that are present on the piezoelectric substrate are a comb-like structure. Voltage is applied at the input IDTs alternately meaning one IDT is given a Voltage supply and another is grounded due to which a wave travels along the surface of the substrate which is because of the inverse piezoelectric effect[4]. The inverse piezoelectric effect is when a mechanical wave or stress is formed on the surface as a result of an electric charge applied. This wave then is received by the output IDT after traveling through the delay path between the input and output IDTs[5]. The delay line or path is the surface present between the input and output IDTs. The output IDTs work on the piezoelectric effect as a result of which electrical response is generated because of mechanical wave received through the piezoelectric substrate. This delay line model of SAW can be used as a sensor when a sensing layer is present on the delay path as can be seen in Fig. 1 (b). This wave traveling through the sensing area is detected at the output IDT as there is a phase change observed due to the perturbation in velocity it undergoes[6]. The telecommunication industry uses SAW delay line mode devices for high-frequency filter designing[7]. SAW delay line models are also used in gas, biological sensors, and devising chemical[8].

There are two ways to build the resonator[9]: either a single IDT with a finite electrode over a piezoelectric substrate or a short IDT with a reflecting grating at the end. Devices with SAW capabilities can be employed as filters, resonators, signal processors, and delay lines between sensors and actuators[10]. When a voltage is given to the electrode, a mechanical wave known as a SAW is excited on a piezoelectric substrate. The IDTsdetermine the frequency of the propagating wave

*Corresponding author: (E-mail: basudeb.ece@nitjsr.ac.in)

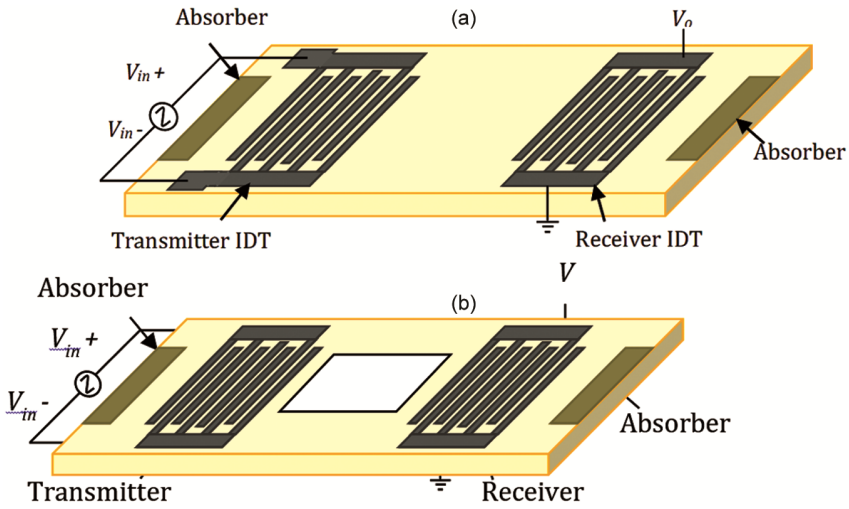

Fig. 1 — (a) SAW Delay line (b) SAW Delay line as sensor.

based on the distance between the two electrodes[11]. Researchers used ZnONano pillars to the sensing area of a two-port delay-line structure to increase sensitivity and the best height of the IDTs to obtain better results for the electrodes was also determined[12]. Researchers conducted a study for sensing C_2H_4 gas as a present for fruit ripening detection. The study offers a sensing layer made up of metal oxides with 0.5µm thickness laid upon $LiNbO_3$ as the substrate for ethylene gas sensing to differentiate the level of maturity of the fruits[13,14]. A substrate made up of $LiNbO_3$ and ZnO nano multilayer structure was projected to boost the performance of the gas sensor. The sensitivity of the sensor may be enhanced because of the increased active surface area which can be gained by changing the aspect ratio of the nanorods, the thinness of the IDT, and the distance between the electrodes[15]. The comparison between a layered sensor with PIB/$LiTaO_3$ and a Multi-layered sensor using PIB/$Al2O_3$/$LiTaO_3$ SAW-based sensor for detection of Di-Chloromethane (DCM) gas[16]. Harathi *et al*. designed a sensor with a sensing layer of zinc oxide to sense the presence of hydrogen gas. The performance was assessed concerning the displacement and the operating frequency in the presence and absence of the testing gas[17]. Omar *et. al*. 2020 designed a sensitivity of polymer-coated SAW-based gas sensors for volatile organic compounds (VOCs). The sensing layers of polymeric materials were taken into consideration because of their properties such as low energy consumption, high sensitivity, performance at room temperature, and short response time on a piezoelectric substrate. The materials that were chosen were polydimethylsiloxane (PDMS), polyisobutylene (PIB), phenylmethyl diphenyl silicone (OV25), polyimide (PI), polyisoprene (PIP). The VOCs chosen for investigation were Dichloromethane (DCM), trichloroethylene (TCE), 1,2-dichloroethylene (DCE), and carbon tetrachloride (CCl4)[17]. Moustafa *et al*. discussed the SAW-based gas sensors for the identification of DCM. The gas sensor response was studied using varying the thickness on five different piezoelectric materials out of which $LiNbO_3$ reported the uppermost resonance frequency[17]. The LN and diamond layers make up the SAW resonator's two-layer construction results from removing the silicon dioxide layer from a three-layered structure, and we discovered a high-quality factor in the outcome. Two-layer structures were shown to have a higher quality factor than three-layer structures. This indicates that the layered complexity is decreased and acquired without a performance impact[18].

S. Trivedi et. al. developed a 3D love wave-based SAW-based gas sensor on 36° YX Lithium Tantalate substrate that serves as the device's waveguide made of SiO_2. Insertion loss and mass sensitivity were noted. The instrument produced a mass sensitivity of 83.22 m2/kg. This was in line with earlier findings[19]. Matthews *et al*. investigated a novel method for analyzing two SAW architectures with varying numbers of electrodes in their IDT and $LiNbO_3$ as the substrate. Then, SAW devices were created based on those calculations, and it was discovered that the measured frequency responses were quite consistent with the results of the simulations[14]. Zhang *et al*. simulated a 3D SAW-based gas sensor for DCM. The substrate is made of $LiNbO_3$, and the sensing layer is made of polyisobutylene (PIB). The selective

adsorption of DCM by PIB from air results in an increase in the bulk of the PIB film. Resonance frequency shifts as a result and is somewhat lowered. So, this sensor can be used to detect DCM[20].

In this article, COMSOL Multiphysics is used to simulate a one-port surface acoustic wave (SAW) resonator. It shows how the interdigital transducer (IDT) and piezoelectric substrate's geometrical structure affect resonance frequency, and simulation is then used to optimize the electrode's height and width. After a thorough investigation that involved adjusting the depth's length and watching its impact on the resonance frequency's nature, the depth of the substrate was chosen. Al was chosen as the material for the electrode while Lithium Niobate was employed as the substrate. Last but not least, a one-port SAW resonator with optimal geometry has been simulated, and both mechanical deformation and electric potential distribution have been recorded. This is highly helpful for modeling any SAW devices[21,22].

2. Device Design and Working Principle

The working theory behind the operation of the sensors is based on Gas adsorption on a surface causes a change in the mass, modulus, and conductivity of the sensing layer, which can be accurately detected using SAW-based gas sensors[6,23] as shown in Fig. 2. To sense hydrogen (H_2) gas, various geometries of SAW-based gas sensors are investigated, constructed, and simulated in the current study. It is observed using frequency shift and displacement plots that the nanorod-based structure showed better sensitivity than the other structure without nanorods. Various materials are considered IDT materials for optimization purposes. Similarly, the height of nanorods is varied to decide the optimum length of the nanorods. Also, the material present in the intermediate layer was varied to see the effects and find a better-resulting model[23].

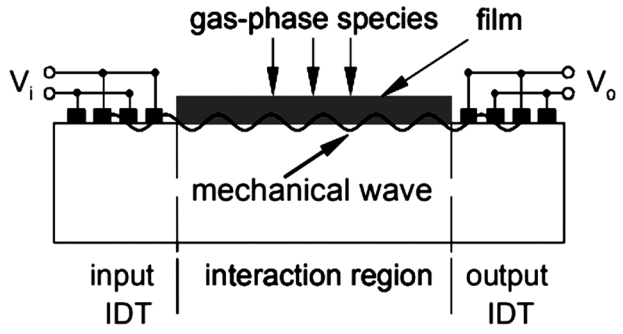

Fig. 2 — Sensing mechanism of the SAW gas sensor.

The operating frequency of the SAW gas sensor depends upon the velocity of the wave (v_0) traveling through the substrate[24]. As the substrate changes the velocity with which the wave travels across the device also changes accordingly. In a delay line model of the SAW gas sensor, the wavelength of a wave is determined using the dimensions of the IDT[25].

$$\lambda=2(W_e + W_{sp}) \quad \ldots(1)$$

Here, "is the wavelength, "W_e" is the width of each electrode, and "W_{sp}" is the distance between each electrode. This then also helps us define the operating frequency of the device. The relation between λ and the operating frequency is as follows

$$f_0 = \frac{v_0}{\lambda} \quad \ldots(2)$$

Here, "v_0" is the propagation velocity of the wave in the piezoelectric substrate, "is the wavelength of the wave, and "f_0" is the operating frequency. The input IDTs are provided with a voltage supply at alternate IDTs. When the sensing layer comes in contact with the gas that is to be detected the properties of the material change. Adsorption of the gas molecules on the layer occurs and causes changes in the frequency of the device. The basic mechanism for the SAW sensors is based on Thermodynamics Equilibrium[26]. The frequency downshift can be calculated by:

$$\Delta f = f - f_0 \quad \ldots(3)$$

Here, f_0 and f are the resonant frequencies for the device before and after exposure togas. $\Delta f$is considereda simple mass load that is attached to the SAW surface as the layer that is formed by the adsorbed gas is thin[27].

$$\Delta f = (k_1 - k_2) {f_0}^2 \rho h \quad \ldots(4)$$

$$\Delta f = (k_1 - k_2) {f_0}^2 \rho h - k2f02\rho \frac{4\mu}{v_0^2}\left\{\frac{\lambda+\mu}{(\lambda+2\mu)}\right\} \quad \ldots(5)$$

Here, $k_1 and k_2$are the coupling constant, "ρ" is the density of the sensing layer which changes after the adsorption of the gas, "h" is the height of the sensing layer, "λ" is the bulk modulus, "μ" is the shear modulus.

3 Modelling of the Gas Sensor

The multilayered nanorod-based Saw gas sensor consists of a piezoelectric substrate, input and output IDTs, an intermediate layer, and nanorods. The most commonly used materials for IDTs are metals such as

Aluminum, Copper, Gold, and Tungsten. Generally, metal oxides such as ZnO, SnO_2, and Al_2O_3 are used as sensing layers in this case nanorods perform this part. Here, in the proposed model we have observed the results for a device with $LiNbO_3$ as a piezoelectric substrate and ZnO material is used for nanorods. The height of the nanorods was varied from 0.05µm to 0.3µm by taking a difference of 0.05µm to obtain the optimized height to get the best results. Also, ZnO and Palladium(Pd)[28] are used as intermediate layers to find which materials presence gives optimized results. The wave velocity *i.e*., the velocity with which the wave travels across the $LiNbO_3$ substrate is 3488 m/s[23]. So here for the device simulation, we have taken "λ" as 4µm. For 2D simulations, we have considered 2 IDTs of 1µm width which are separated by 1µm of distance. The thickness of the IDTs is 0.02 µm. The intermediate layer is taken as 0.2µm of thickness. The height of the substrate is taken as "5λ" which means 20µm for this model.

Figure 3 shows the 2D basic structure of a unit cell for a nanorod-based SAW gas sensor. The results are obtained by varying the intermediate layer materials, changing the height of the nanorods, and altering the materials of IDT. Simulation for a 2D model was done for a device with a length of 4µm and height of 8µm. The material used for the substrate is $LiNbO_3$, while ZnO is used for nanorods structure and IDT is made up of Aluminum. Simulation using the above materials is done by changing the intermediate layer's material.

3.1 Steps to model in COMSOL Multiphysics

The basic steps to create the basic Saw based gas Sensor are as follows:

i. Input the parameters of the materials to be used for the sensor.

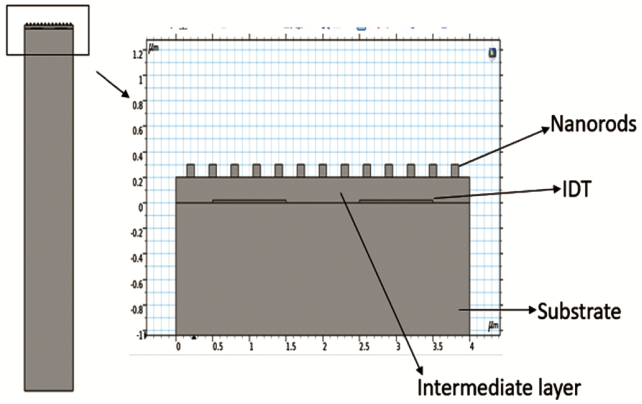

Fig. 3 — The 2-D Geometry of the SAW unit cell with nanorods.

ii. Create the physical components for the sensor with the required dimensions.
iii. Define properties of the materials like piezoelectric materials, *etc*.
iv. Assign the materials for each component and also enter the accurate values for the used materials.
v. Define the exact conditions for the produced structure of the sensor
vi. Construct a mesh by defining the accurate values.
vii. Set up a parametric sweep to solve the model with and without the adsorbed species on the sensor.
viii. Plot the graph and by properly adjusting the deformed wave plot see the effect.
ix. The eigenfrequency values can be seen in the results which show values before and after exposure to the gas.

3.2 Simulation Methodology

For $LiNbO_3$the velocity of the wave through it is 3488m/s. The values of the Piezoelectric substrate required for simulation are as follows[11]:

$$C=\begin{pmatrix} c_{11} & c_{12} & c_{13} & c_{14} & 0 & 0 \\ c_{12} & c_{11} & c_{13} & -c_{14} & 0 & 0 \\ c_{13} & c_{11} & c_{33} & 0 & 0 & 0 \\ c_{14} & -c_{14} & 0 & c_{44} & 0 & 0 \\ 0 & 0 & 0 & 0 & c_{44} & c_{14} \\ 0 & 0 & 0 & 0 & c_{14} & (c_{11}-c_{12})/2 \end{pmatrix} \quad ...(6)$$

$$e=\begin{pmatrix} 0 & 0 & 0 & 0 & e_{15} & -e_{15} \\ -e_{22} & e_{22} & 0 & e_{15} & 0 & 0 \\ e_{31} & e_{31} & e_{33} & 0 & 0 & 0 \end{pmatrix} \quad ...(7)$$

$$\varepsilon=\begin{pmatrix} \varepsilon_{11} & 0 & 0 \\ 0 & \varepsilon_{11} & 0 \\ 0 & 0 & \varepsilon_{33} \end{pmatrix} \quad ...(8)$$

Here, C: Elasticity Matrix, e: piezoelectric Constants, ε: Dielectric Constants.

For the simulation process, we have considered $LiNbO_3$ as a piezoelectric substrate so, the values for the same are as given in Table 1:

After assigning the materials itsvalues, we assign one IDT with an input voltage of 1V and another IDT as ground.

The summary of boundary conditions for the 2D model used in the simulation is given in Table 2:

We perform eigen frequency analysis on the model to find out what is the resonant frequency and anti-resonant frequency for the device. Resonant frequency generally refers to the frequency when the displacement obtained is maximum for that material. We also observed the displacement of the device

Table 1 — Properties of Lithium Niobate ($LiNbO_3$)

Dielectric Constant	ε_{11}	85.2
	ε_{33}	28.7
Elastic Constants ($\times 10^{11}$ N/m^2)	c_{11}	2.03
	c_{12}	0.573
	c_{13}	0.752
	c_{14}	0.085
	c_{33}	2.424
	c_{44}	0.595
Piezoelectric Strain Constants(C/m^2)	e_{15}	3.7
	e_{22}	2.5
	e_{31}	0.23
	e_{33}	1.33
Crystal Density(kg/m^3)	ρ	4.647 x 10^3

Table 2 — Solid Mechanics Condition for the model

Name	Mechanical Boundary Condition
Side 1, Side 2, Plane 2	Continuity /Periodic Condition
Plane 1	Antiperiodic Condition
Side 3, Plane 3	Fixed Constraint

using frequency and time-dependent analysis. We observed the difference in the frequency in the absence and presence of the gas to be detected. The model used to find out these frequencies consists of a Piezoelectric substrate upon which IDTs are placed.

4. Results and Discussion

4.1 2-D-based Device Structure

Various graphs are obtained after simulation of the model in 2 dimensions. The results obtained are by simulating the proposed model using eigen frequency, Time-domain, and Frequency-domain analysis methods.

Figure 4 shows the meshing structure for a basic one-port SAW gas sensor with and without the presence of nanorods. The meshing done in this 2D environment is physics-controlled. Fine meshing is used to obtain more accurate results.

Figure 5 (a) shows the plot for a surface profile of resonant frequency for the device. The figure shows that the displacement observed at IDT is minimal while that around the IDTs can be seen to be maximum. The Fig. 5(b) shows the anti-resonant frequency plot for the nanorods-based SAW device. The output above is obtained using the eigen frequency study. We can observe at anti-resonant frequency the displacement at IDT is maximum and that around the IDTs is reduced.

Figure 6 above shows the time analysis graph for a 2D model of the nanorod-based gas sensor with 0.25µm nanorod height. The above plot obtained is at

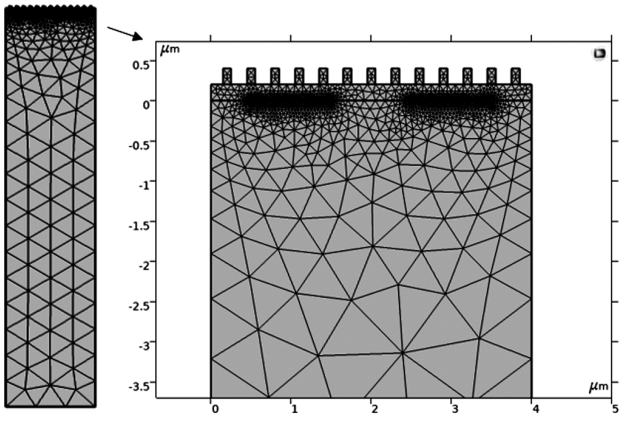

Fig. 4 — Mesh structure of ZnO Nanorod-based SAW Gas Sensor.

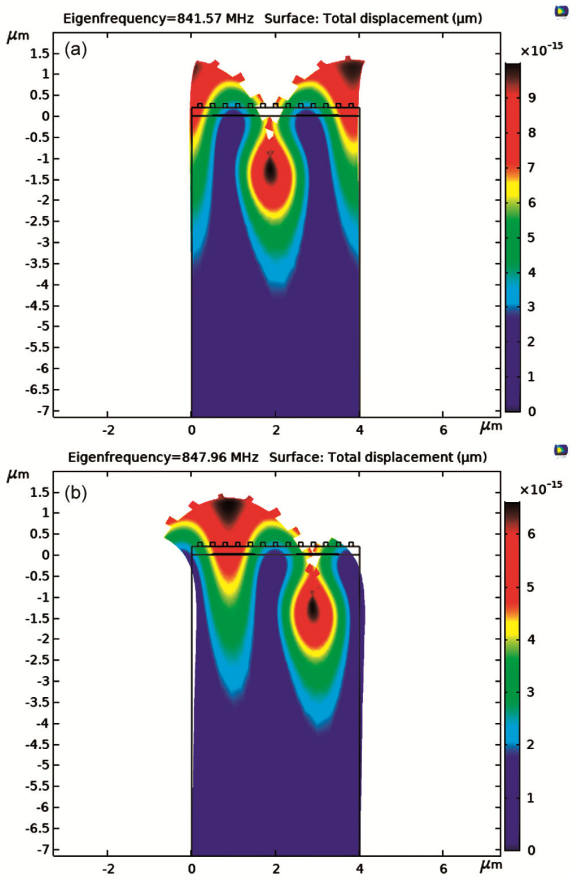

Fig. 5 — Mesh structure of ZnO Nanorod-based SAW Gas Sensor.

the input IDT side where the input is given to that IDT is 1V. The Above figure shows the displacement behavior of the sensor concerning time. The above output result is obtained with the help of a time domain study. In this analysis, the model was tested for some time to sense the gas molecules.

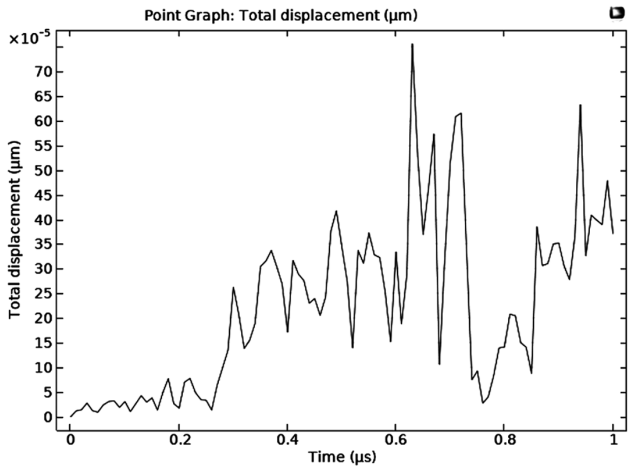

Fig. 6 — Time Analysis for the proposed 2-D structure model.

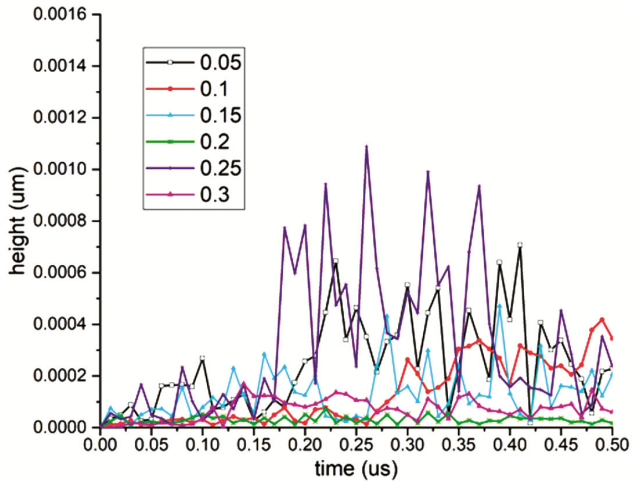

Fig. 7 — Time Analysis graph for various nanorod heights.

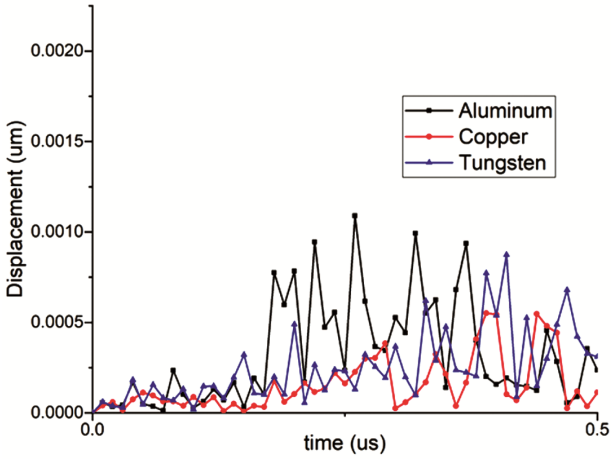

Fig. 8 — Time Analysis graph after varying IDT materials.

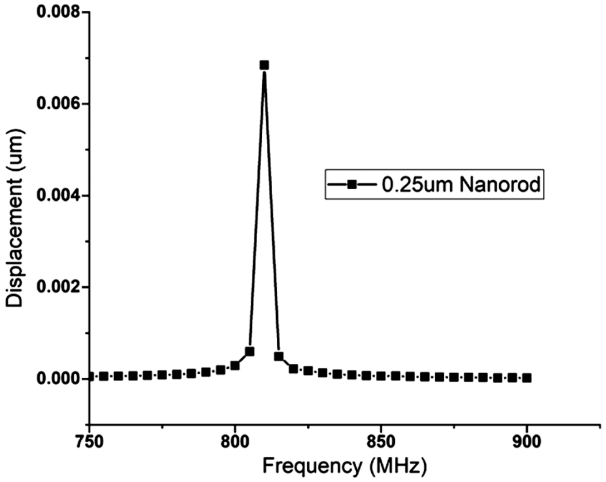

Fig. 9 — Frequency Analysis graph for 2-D structure.

Figure 7 shows the displacement graph at the input IDT point for nanorod-based SAW gas sensor models with a varying height of nanorods. We can observe from the above graph the displacement versus time plot for models with nanorods of height 0.05µm, 0.1 µm, 0.15 µm, 0.2 µm,0.25 µm, and 0.3 µm. Fromthe above graph itself, we can see that the displacement for a model with a nanorod height of 0.25 µm is maximum. This indicates the absorption of the gas molecules and sensitivity of the sensor will be optimum with the use of 0.25 µm nanorod on the surface of the piezoelectric substrate.

Using previous graph information, we observed that the 0.25 µm height nanorod model had maximum displacement so we performed time analysis on the same model by varying the IDT materials. We observed the graph outputs for Aluminum, Copper, and Tungsten. Fig. 8 shows the time analysis displacement versus the time graph for the 0.25 µm height nanorod model with varying IDT materials. From the above graph, we can conclude that Aluminum material when used as IDT shows maximum Displacement. Hence a combination of aluminum material of height 0.25 µm nanorod will produce the optimum result.

Figure 9 shows the graph obtained using frequency domain analysis. As we can observe the displacement versus frequency graph is plotted and the maximum displacement is seen to be at the resonant frequency for that model. The above figure is a plot observed for a 0.2 µm height nanorods-based model.

Figure 10 shows the Frequency versus displacement graph for models with varying nanorod height from 0.05 µm to 0.3 µm with a 0.05 µm difference. It can be observed that as the height of the nanorod changes the resonant frequency changes accordingly the frequency where maximum displacement is gained also varies. The above graph is obtained using a Frequency analysis study.

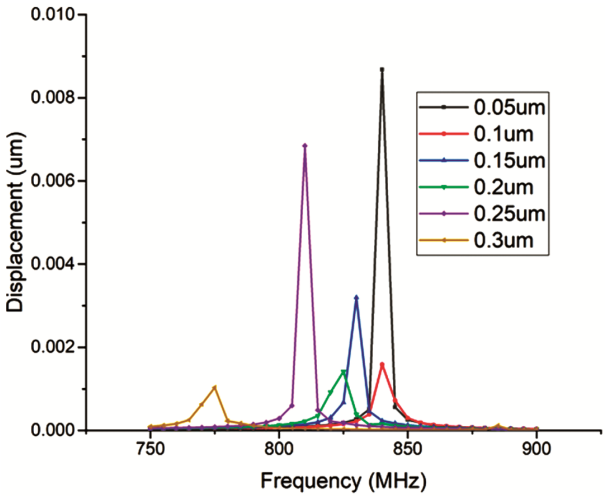

Fig. 10 — Frequency Analysis graph for 2-D structure for various Nanorod heights.

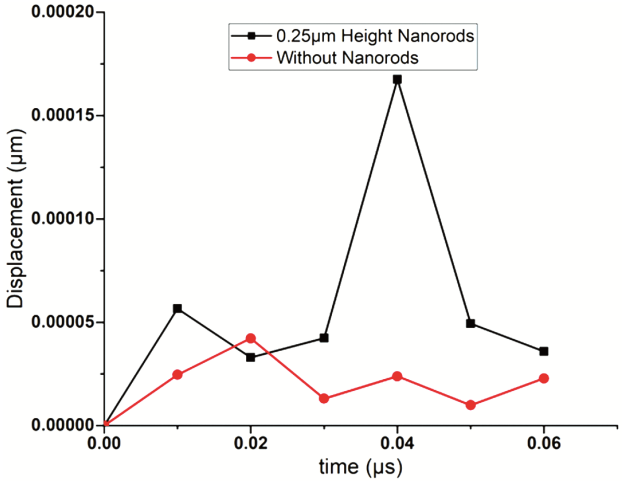

Fig. 11 — Displacement Vs Time Plot for SAW gas sensor with and without nanorods.

4.2 Comparison between SAW gas sensors with and without Nanorods

The plots in Fig. 11 show the displacement plot comparison between SAW-based gas sensors with and without nanorods in time domain analysis for the surface of the SAW-based Gas sensor. The graph indicates that the displacement observed in the nanorod-based structure is better than the SAW gas structure without nanorods. Thus, we can say that the addition of nanorods to the structure has improved the sensitivity of the SAW gas sensor.

4.3 3-D environment-based device structure

The gas sensor was realized through a 3D environment in COMSOL Multiphysics. The meshing structure is reported in the Fig. 12.

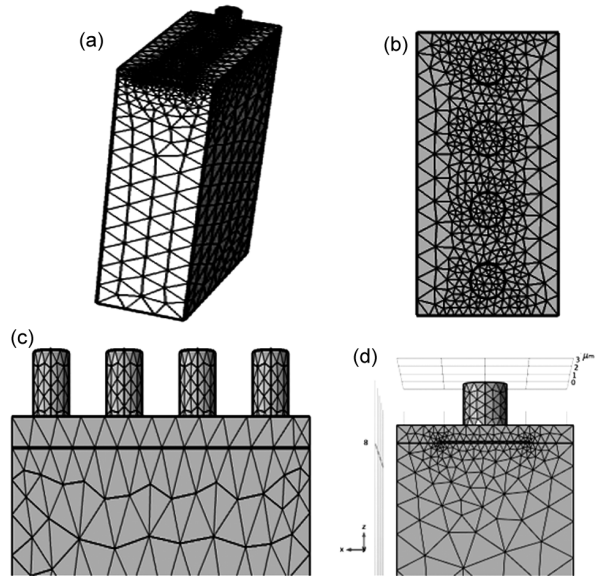

Fig. 12 — Mesh for 3-D model (a) Mesh structure of ZnO nanorod-based SAW Gas Sensor (b) XY Plane mesh (c) YZ Plane mesh (d) XZ Plane mesh.

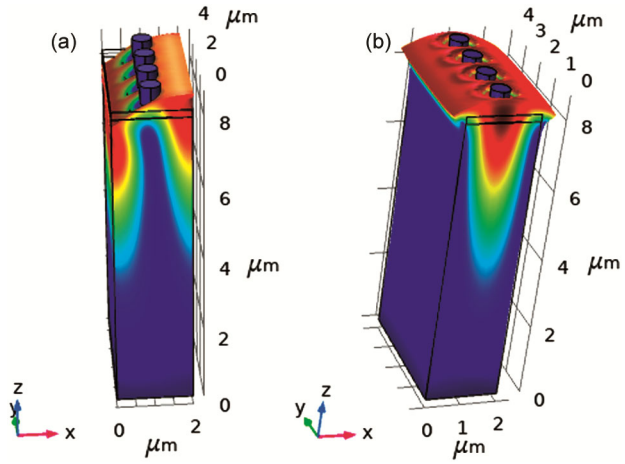

Fig. 13 — Displacement magnitude of (a) resonant, (b) anti-resonant frequency.

Figure 13 shows the displacement plot concerning time using the time domain study for the 3D model of the nanorod-based SAW gas sensor. The plots in Fig. 13 show the deformed shape plot for the surface of the SAW-based Gas sensor having nanorods height of 0.5µm for the value of the first Eigen frequency value which is the resonant frequency for the device is 852.47 MHz. and the second Eigen frequency value is anti-resonant frequency is 861.85 MHz. respectively. For the above model, $LiNbO_3$ was the piezoelectric substrate, aluminum was used as IDT material and ZnO was used as both the intermediate layer as well as for nanorods.

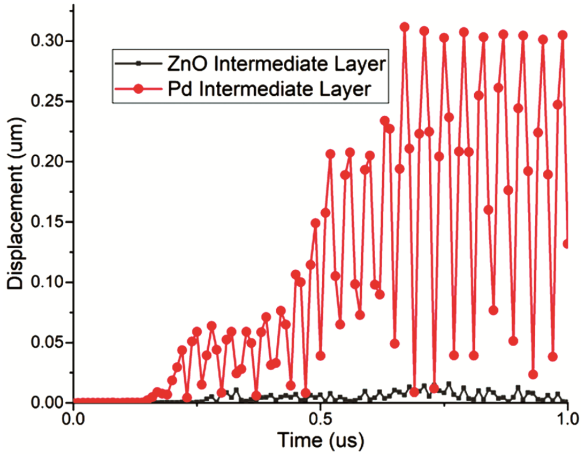

Fig. 14 — 3-D structure Time Analysis comparison for ZnO and Pd intermediate layers.

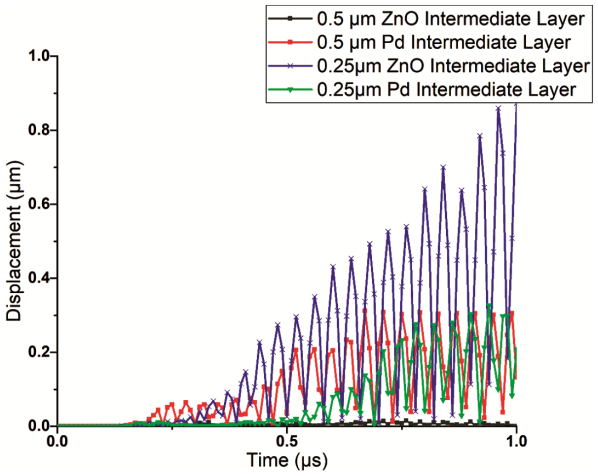

Fig. 15 — Comparison graph of different layers of ZnO and Pd material.

The above graph in Fig. 14 depicts the displacement plot for a 3D model using Time domain analysis. The above graph is obtained for the model where the piezoelectric substrate was $LiNbO_3$, IDT material was aluminum, the Intermediate layer was Palladium and the material used for nanorods was ZnO. The above figure shows the comparison of displacement at input IDT for two nanorods-based SAW gas sensor models where the intermediate layers are different. We can observe from the above plot that displacement obtained by using Palladium as an intermediate layer significantly improved the displacement graph for that model sensor.

Figure 15 shows the comparison of displacement at input IDT for two nanorods-based SAW gas sensor models where the intermediate layers are ZnO and Pd, and for the nanorods, height is 0.25µm and 0.5µm.

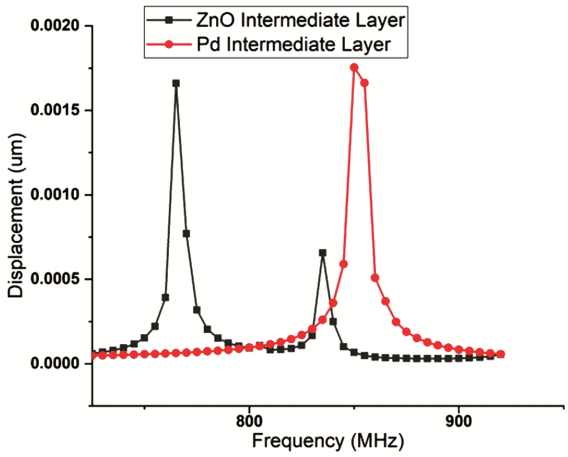

Fig. 16 — Frequency Analysis graph for various nanorod heights.

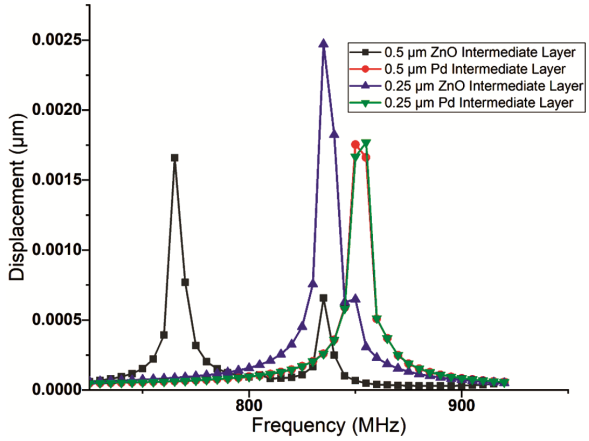

Fig. 17 — Frequency Analysis for various heights of ZnO and Pd material Nanorod.

We can observe from the above plot that displacement for ZnO as an intermediate layer when the height of nanorods is 0.25µm significantly improved the displacement graph for that model sensor. Hence a combination of ZnO of height 0.25 µm nanorod will produce the optimum result.

The above graph is obtained using a frequency domain study which gives us a Frequency versus displacement plot. Observing the above graph, we can say that the displacement for the model is maximum at its resonant frequency. Fig. 16 shows frequency domain analysis for two models one using ZnO as an intermediate layer while another using Pd as an intermediate layer. The above Fig. 16 is a plot observed for 0.5µm height nanorods-based SAW gas sensors in the 3D model where the intermediate layer is Palladium.

The above graph in Fig. 17 is obtained using a Frequency domain study which gives us a Frequency

versus displacement plot. Observing the above graph, we can say that the displacement for the model is maximum at its resonant frequency. Figure shows frequency domain analysis for two models one using ZnO as an intermediate layer while another using Pd as an intermediate layer and varying nanorod heights of 0.25 µm and 0.5µm.

5 Conclusion

Initially, various literature surveys were presented on the gas sensor. Then the construction, working principle, and simulation methodology of the proposed sensor are presented. 2 D and 3D-based Nanorod-based SAW gas sensor simulation is presented. It is observed that when there is a change in the IDT material and intermediate material the displacement graph changes accordingly. The results were obtained for frequency domain analysis and time domain analysis with varying the height of the nanorod. The maximum displacement of the SAW gas sensor was observed for a model with 0.25µm nanorod height on the surface. In the 2D simulation, it is concluded that a combination of aluminum material of height 0.25 µm nanorod will produce the optimum result. In 3D analysis, the combination of ZnO of height 0.25 µm nanorod produces the optimum result. The comparison results show that the nanorod-based structure is better than the SAW gas structure without nanorods. Thus, we can say that the addition of nanorods to the structure has improved the sensitivity of the SAW gas sensor. Basically, from the simulation and analysis of the SAW gas sensor, it is concluded that this sensor can be used for the detection of volatile gases.

References

1 Auld B A, *Acoustic Fields and Waves in Solids,1st Edn* Stanford, California: John Wiley & Sons Publication, 1 (1973).

2 Behera B, *Modelling, Simulation and Fabrication of Surface Acoustic Wave Motors Employing Dual Friction- drive*, Indian Institute of Technology Guwahati, India, 2016.

3 Behera B, Nemade H B & Trivedi S, *IEEE Int Ultra Symp*, Tours, France, (2016) 1.

4 Behera B & Nemade H B, *Procedia Eng*, 144 (2016) 1411.

5 Behera B & Nemade H B, *Ferroelectr Lett Sect*, 45 (2018) 8.

6 Tiwary A, Kumar J & Behera B, *Phys B Condens Matter*, 669 (2023) 415279.

7 Turuk B K & Behera B, *Ferroelectrics*, 615 (2023) 132.

8 Tiwary A, Pradhan S, Kumar J & Behera B, *5th Int Conf Electr Comput Commun Technol,* 2023 (2023) 1.

9 Mamishev A V, Rajan K S, Yang F, Du Y & Zahn M, *Proc IEEE*, (2004) 808.

10 Royer D, *Elastic waves in solids 1*, 1996.

11 Behera B, *Sensors Actuators A Phys*, 331 (2021) 1.

12 Plessis H G & Perold W J, *Proc COMSOL*, (2013) 1.

13 Hasanuddin N H, *et al.*, *3rd Int Conf Electron Des ICED 2016*, (2017) 52.

14 Kabir K M M, Matthews G I, Sabri Y M, Russo S P, Ippolito S J & Bhargava S K, *Smart Mater Struct*, 25 (2016).

15 Hasan M N, Maity S, Sarkar A, Bhunia C T, Acharjee D & Joseph A M, *J Electron Mater*, 46 (2017) 679.

16 Gupta A, Kumar P & S Pandey, *Proc - Int Conf Trends Electron Informatics, ICEI 2017*, (2018) 239.

17 Harathi N, Kavitha S & Sarkar A, *Mater Today Proc*, 33 (2020) 2621.

18 Turuk B K & Behera B, *Mater Today Proc*, 56 (2022) 883.

19 Trivedi S & Nemade H B, *Excerpt from Proc 2015 COMSOL Conf Pune*, 1 (2015) 2.

20 Rao Y L & Zhang G, 3-D Modeling of Surface-Acoustic-Wave Based Sensor, *COMSOL*, 2007.

21 Nagmani A K, Turuk B K & Behera B, *AIP Conf Proc*, 2341 (2021) 020043

22 Behera B, *IEEE Sens J*, 19 (2019) 1.

23 Tiwary A, Rout S S & Behera B, *Trans Electr Electron Mater*, (2022) 1.

24 Soloman S, *Sensors Handbook*, (2010).

25 Morgan D, *Surface Acoustic Wave Filters With Applications to Electronic Communications and Signal Processing*, 2nd Edn Oxford: Elsevier Academics Press, (2007).

26 Ho C K, Lindgren E R, Rawlinson K S, McGrath L K & Wright J L, *Sensors*, 3 (2003) 236.

27 Moustafa M, Laouini G, ElNaggar M & AlZoubi T, *Ferroelectrics*, 572 (2021) 94.

28 Akshya S & Juliet A V, *Sci Rep*, 11 (2021) 1.